Organic LETTERS

Letter

pubs.acs.org/OrgLett

Exclusive Hydrophobic Self-Assembly of Adaptive Solid-State Networks of Octasubstituted 9,9′-Spirobifluorenes

Lidia Pop,[†] Florina Dumitru,[‡,§] Niculina D. Hădade,[†] Yves-Marie Legrand,[‡] Arie van der Lee,[‡] Mihail Barboiu,*[,‡] and Ion Grosu*[,†]

[†]Supramolecular Organic and Organometallic Chemistry Center (SOOMCC), Babes-Bolyai University, 11 Arany Janos str., 400028 Cluj-Napoca, Romania

[‡]Adaptive Supramolecular Nanosystems Group, Institut Européen des Membranes − ENSCM-UMII-CNRS 5635, Place Eugène Bataillon, CC 047, F-34095 Cedex 5 Montpellier, France

[§]Department of Inorganic Chemistry, Physical Chemistry and Electrochemistry, University Politehnica of Bucharest, 1, Polizu st., RO-011061 Bucharest, Romania

Supporting Information

ABSTRACT: An easy and powerful access to 3,3′,6,6′-tetrasubstituted 9,9′-spirobifluorene derivatives with tetrahedral orientation of the peripheral groups (i.e., −I, −CN, $-NO_2$, −CH═O, −COOH, −C≡CH, −4-Py) was developed. The NMR and HRMS results are in agreement with the proposed formula and the solid-state molecular structures obtained by single-crystal X-ray diffraction. They form molecular solids self-assembled via exclusive hydrophobic interactions. Solid-state selection and adaptation can be obtained on the basis of variable compact packing of functional groups present on the 9,9′-spirobifluorene backbone.

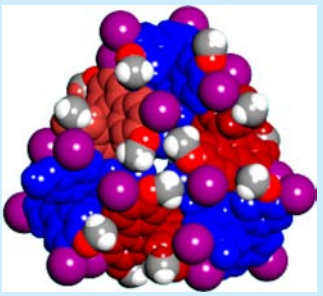

Hydrophobic interactions are of fundamental importance for many biological functions. The spatial positioning of hydrophobic residues within the proteins can determine their architectures and folding behaviors.[1] Because of the great significance of these processes, design of synthetic artificial superstructures, exclusively driven by the hydrophobic effects, has become an area of expanding interest.[2] Related approaches are based on lipophilic systems showing efficient integrated self-assembly, but the prediction of the final superstructures remains challenging.[3] Directional forces (i.e., H-bonding, electrostatic or coordination interactions, etc.) are the most important driving forces that induce the self-assembly of artificial superstructures. For most artificial systems, directional interactions play an important role in reinforcing the dissipative hydrophobic self-assembly.[4] However, artificial superstructures based on unique hydrophobic contacts remains rare.

Within this context, the 9,9′-spirobifluorene backbone constituted from two fluorene units joined through a shared spiro carbon[5−8] represents an unusual structural motif, shedding light on unique opportunities for investigating a variety of fundamental aspects of hydrophobic self-assembly. The 9,9′-spirobifluorene derivatives present a D_{2d} point symmetry, with an Onsager cruciform rigid spatial arrangement.[7a] Their single-crystal structures show that 9,9′-spirobifluorene aggregates through short (3.22−3.45 Å) intermolecular edge−edge π-aromatic interactions[7b] or via the C−H···π(arene) interactions.[8] The functionalization of the aromatic units of the 9,9′-spirobifluorene platform results in the formation of porous molecular solids with significant porosity (44−60%) for the inclusion of guests[9] or of polymers with intrinsic microporosity (PIMs).[10] Other applications are enantioselective recognition and catalysis[11] or organic light-emitting diodes (OLED) technology.[12]

Herein, we report a series of 2,2′,7,7′-tetramethoxy-3,3′,6,6′-substituted-9,9′-spirobifluorenes **3**−**12** (substituents: −I, −CN, $-NO_2$, −CH═O, −COOH, −C≡CH, −4-pyridine) (Scheme 1). Four of these compounds (**3**, **5**, **7**, and **11**, Scheme 2a) were crystallized, and their structures determined by single-crystal X-ray diffraction revealed that they adaptively form self-assembled molecular solids via exclusive weak hydrophobic interactions.[13] Their simultaneous self-assembly encodes the supramolecular guiding information on the orthogonal arrangement of the rigid fluorene units and the specific molecular packing of various substituents grafted on an aromatic backbone, which adaptively fill the available space with a very compact packing within the network.

Our primary efforts were concentrated on developing novel and powerful methods for the synthesis of tetrahedral 2,2′,7,7′-tetramethoxy-3,3′,6,6′-substituted-9,9′-spirobifluorenes **3**−**12** by using methoxy (CH_3O−) *ortho*-directing groups in the 2,2′,7,7′ positions. The chemically inert CH_3O− moieties may assist halogenation in the 3,3′,6,6′ positions, which may be used for a series of further substitution reactions. The synthetic strategy implied in the first step is the transformation of 9,9′-spiro-bifluorene, quantitatively, with I_2/bis[(trifluoroacetoxy)-

Received: May 29, 2015
Published: July 7, 2015

DOI: 10.1021/acs.orglett.5b01576
Org. Lett. 2015, 17, 3494−3497

Scheme 1. Synthetic Scheme for the Formation of Compounds 2−9 from Compound 1

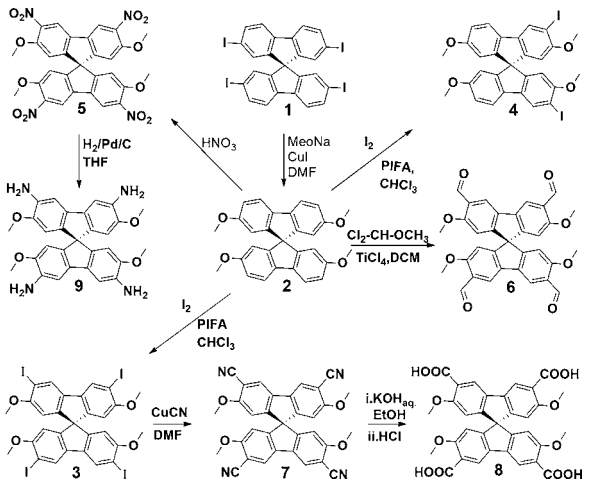

Scheme 2. Synthetic Scheme for the Formation of Compounds 10−12 from Compound 3

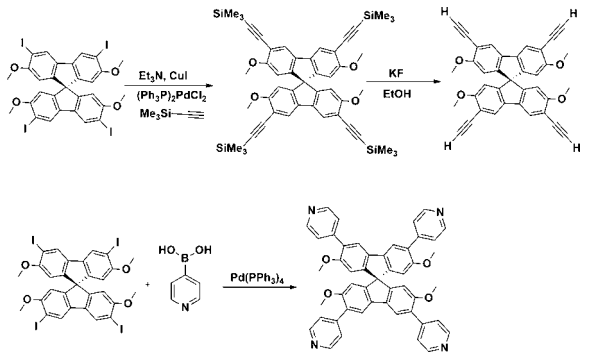

iodo]benzene−PIFA in $CHCl_3$ into the tetraiodinated derivative **1**.[14] The compound **1** in reaction with MeONa and CuI in DMF/MeOH yielded the 2,2′,7,7′-tetramethoxy-spiro-bifluorene **2**. The iodination of **2** under similar conditions (I_2/PIFA in $CHCl_3$) yielded the tetraiodinated (**3**) and the diiodinated (**4**) derivatives, respectively, depending on the selected molar ratios of **2**:I_2:PIFA. The nitration of **2** regioselectively yields (85%) the tetranitro derivative **5**, while the $TiCl_4$-catalyzed formylation of **2** with Cl_2CHOCH_3 gave (40% yield) the tetraformyl derivative **6** (Scheme 1). The tetracyano derivative **7** was obtained starting from **3** by classic substitution of iodine with CuCN in DMF (79% yield). The hydrolysis of cyano groups was carried out with KOH in ethanol and then acidulation with HCl led to tetracarboxylated derivative **8** (75% yield). The reduction of the tetranitro derivative **5** with H_2, over Pd/C as catalyst, led to the tetraamino compound **9** (87% yield) (Scheme 1). This optimized procedure of only four steps instead of seven with considerably better overall yields (65% instead of 20%) represents a simplified alternative to previous reports[9,15] for the synthesis of 3,3′,6,6′-tetraamino-9,9′-spiro-bifluorene derivatives. To obtain the tetraethynyl-spiro-bifluorene**11**, the Sonogashira cross-coupling reaction provided compound **10** (51% yield), while the deprotection reaction was almost quantitative (95% yield) (Scheme 2a). The Suzuki−Miyaura cross-coupling reaction of **3** with the 4-pyridylboronic acid gave the tetrapyridyl-spirobifluorene **12** (38% yield) (Scheme 2b).

The structures of compounds **2**−**12** were confirmed by ^1H and ^{13}C NMR spectra, positive ES-HRMS measurements (Supporting Information), and single-crystal X-ray diffractometry.The pattern of the ^1H NMR spectra for the tetrasubstituted compounds **3** and **5**−**12** contains three singlets with a ratio of the intensities of 3/1/1 situated in the range 3.7−3.9 (OCH_3), 6.8−6.9 (4-H, 4′-H, 5-H, 5′-H), and 7.5−7.6 (1-H, 8-H, 1′-H, 8′-H). The expected ^1H NMR spectra of compound **4** and its regioisomer **iso-4** (Figure 1) are similar and exhibit three singlets

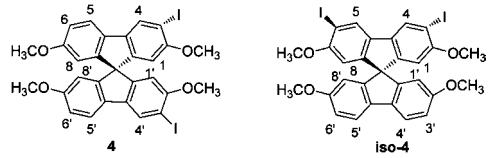

Figure 1. Chemical representation for compound **4** and its regioisomer **iso-4**.

(**4**: 4-H, 4′-H; 1-H, 1′-H and 8-H, 8′-H; **iso-4**: 4-H, 5-H; 1-H, 8-H and 1′-H, 8′-H) and two doublets (**4**: 5-H, 5′-H and 6-H, 6′-H; **iso-4**: 4′-H, 5′-H and 3′-H, 6′-H). The ROESY spectrum of **4** revealed a correlation between the singlet (δ = 8.12 ppm) of the H_4 and $H_{4'}$ protons and the doublet (δ = 7.59 ppm) of the $H_5$and $H_{5'}$ protons, confirming the formation of compound **4** inside its isomer **iso-4**.

The X-ray single-crystal structures of the compounds **3**, **5**, **7**, and **11** were determined using crystals obtained by slow diffusion of diethyl ether or diisopropyl ether in dichloromethane solutions at room temperature (Figures 1−4). The X-ray diffraction reveals as a general feature the rigid spiro-backbone of octasubstituted 9,9′-spirobifluorene with two orthogonal fluorene units bearing CH_3O− groups in positions 2,2′,7,7′ and different electron-withdrawing substituents (−I, −C≡N, $-NO_2$, −C≡CH) in positions 3,3′,6,6′. In all structures, the octasubstituted 9,9′-spirobifluorenes present distortions in angles from the ideal sp^3 hybridization geometry around the central C atoms, probably as a consequence of the strain imposed by the fluorene rings and the indirect steric effects. The dihedral angles between the fluorene rings range from 87.89 to 89.78°, calculated for all of the residues in the asymmetric units of the crystal structures. However, despite the structural similarity of the core backbone of the 9,9′-spirobifluorene compounds, their interactions patterns and crystal packing are very different: **3**, **7**, and **11** crystallize in achiral space groups *P*-1, *Pbca*, and $P2_1/c$, respectively, while remarkably, **5** crystallizes in the chiral space group $P4_3$.

Symmetry expansion of the crystal cell shows that the self-assembly of the monomeric units forms tetrameric and hexametric aggregates of different dimensions and shapes: triangular hexamers for **3** (Figure 2), extended hexagonal hexamers for **5** (Figure3), squared tetramers for **7** (Figure 4), and star-type hexamers for **11** (Figure 5).

As a very interesting feature, the self-assembly is not based on any specific/classic directional interactions such as hydrogen-bonding, aromatic stacking, or electrostatic interactions. Interweaved peripheral aromatic rings are in van der Waals contact in a one-over/one-under fashion. Multiple aromatic hydrophobic contacts between the external hypersurfaces of the molecules are ubiquitous, strongly contributing to the cohesion of the self-assembled aggregates. Embrace motifs are formed between the aromatic units within the interstices between molecules so that their internal available space is filled. Aromatic

DOI: 10.1021/acs.orglett.5b01576
Org. Lett. 2015, 17, 3494−3497

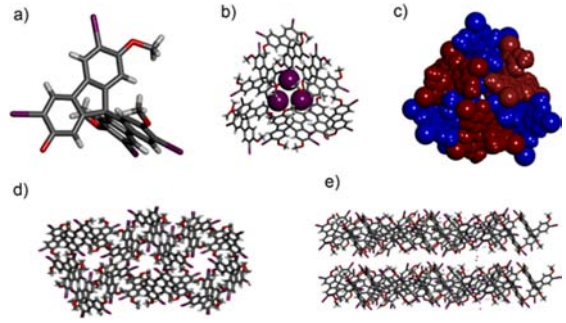

Figure 2. Crystal structure of (a) molecular synthon **3** and of the associated hexamers $\mathbf{3}_6$ in (b) stick and (c) CPK representations; (d) top and (e) side view of the crystal packing of **3**.

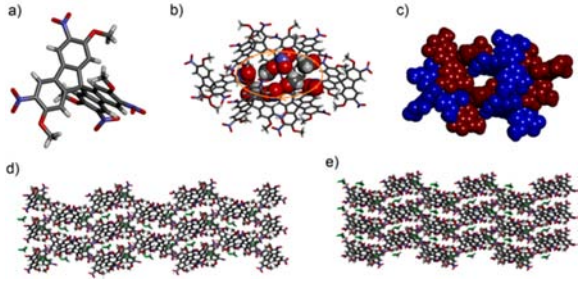

Figure 3. Crystal structure of (a) molecular synthon **5** and of the associated hexamers $\mathbf{5}_6$ in (b) stick and (c) CPK representations; (d) top and (e) side view of the crystal packing of **5**.

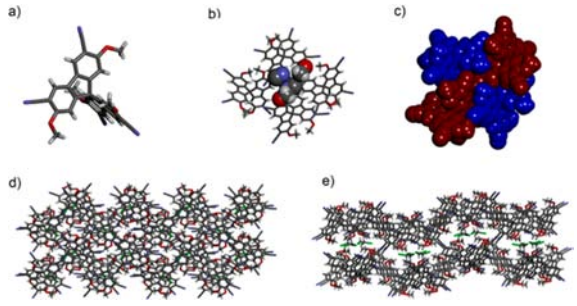

Figure 4. Crystal structure of (a) molecular synthon **7** and of the associated tetramers $\mathbf{7}_4$ in (b) stick and (c) CPK representations; (d) top and (e) side view of the crystal packing of **7**.

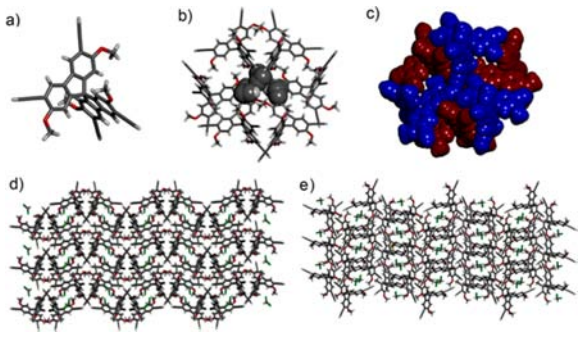

Figure 5. Crystal structure of (a) molecular synthon **11** and of the associated hexamers $\mathbf{11}_6$ in (b) stick and (c) CPK representations; (d) top and (e) side view of the crystal packing of **11**.

embrace motifs are well documented for a series of aromatic clusters,[16,17] and their significance in terms of interactions (stabilization energy of the benzene trimer is estimated to be −20 kJ/mol) is widely recognized.[18]

At this point, an important question arises: what are the structural insights and contributions to the generation of such diversity of geometrically/constitutionally variable architectures since they result from the hydrophobic aggregation of structurally similar platforms? A very important structural detail is related to dipolar interactions between the electron-donor CH_3O- groups and the grafted electron-acceptor −I, $-C{\equiv}N$, $-NO_2$, and $-C{\equiv}CH$ groups. Within this context, we discovered that the dipolar groups (−I, $-C{\equiv}N$, and $-C{\equiv}CH$) are oriented toward the center of the supramolecular hexameric or tetrameric structures, respectively, while the CH_3O dipolar groups surround the positions around the circular cavities. They are strongly dependent on the nature, geometry, and spatial orientation of the interacting dipolar groups: two oppositely oriented dipoles for $-C{\equiv}N$ groups, three iodine atoms, and six acetylene groups. It may be considered as an important structural factor that could further differently express the relative spatial orientation of the 9,9′-spirobifluorene platforms and, thus, their solid-state packing. The supramolecular information encoded in these dipolar inner interactions is related to specific localized steric and structural interactions between these substituents. As a consequence, the compounds **3**, **5**, **7**, and **11** are not isostructural and display very different unit cells and packing arrangements.

The 9,9′-spirobifluorenes **3**, **7**, and **11** are organized in crystal so that each successive molecule has an alternate opposite chirality. Overall, the crystal is racemic: homochiral monomers of opposite chirality are stratified.

The electronic nature and geometrical behavior of the $-NO_2$ group do not allow the specific central packing observed for −I, $-C{\equiv}N$, $-C{\equiv}CH$ groups, which are packed in the central part of the structure in symmetric arrangements. Therefore, the ability of the $-NO_2$ group to steer the packing of **5** is amazingly different. Accordingly, the $-NO_2$ and CH_3O- are packed in a chiral dissymmetric supramolecular arrangement in the central part of the hexagonal architecture (Figure 3b). Similarly, in the crystal, each 9,9′-spirobifluorene of one chirality interacts with six other molecules of the same chirality so that each molecule presents a tight contact. This results in the propagation of the homochirality with the formation of a chiral crystal as we have previously observed for double-helical architectures obtained from achiral ligands and metallic ions.[19]

The hydrophobic packing invariable quartet and hexameric motifs imposes a series of lamellar arrays in which the spirofluorene molecules run in two nearly perpendicular directions to generate the mesh interweaved layers (Figures 1−4d,e).

In conclusion, these results demonstrate that the weak hydrophobic interactions, rather unconventional and so far partially reduced option for multiple coding of the self-assembly processes of artificial systems, are very powerful for generating compact architectures in the solid state. Molecular information confered by 9,9′-spirobifluorenes is promoted at the supramolecular level via the molecular packing of various substituents of variable geometry and polarity orienting the external van der Waals hypersurfaces of the molecules for further interactions in a very adaptive way. Crystallization adaptively favors the formation of tetrameric or hexameric clusters that allow closer molecular packing, thereby optimizing the hydrophobic interactions. The homochirality in the solid state of compound **5** is promoted by asymmetric spatial arrangementof molecular substituents positioning the 9,9′-spirobifluorene platforms to interact via their

DOI: 10.1021/acs.orglett.5b01576
Org. Lett. 2015, 17, 3494−3497

external van der Waals hypersurfaces in the supramolecular hexamers of the same chirality. The robustness of the multivalent hydrophobic contacts is responsible for the transmission of the supramolecular homochiral order. Similar packing processes between chiral biosurfaces control the functions of the gramicidin A ion channel,[20a] the self-assembly of collagen fibers,[20b] and tobacco mosaic virus.[20c]

■ ASSOCIATED CONTENT

Supporting Information

Experimental procedures, ^{1}H and ^{13}C NMR spectra, ES-HRMS spectra, and X-ray diffraction. The Supporting Information is available free of charge on the ACS Publications website at DOI: 10.1021/acs.orglett.5b01576.

■ AUTHOR INFORMATION

Corresponding Authors

*E-mail: mihail-dumitru.barboiu@univ-montp2.fr.
*E-mail: igrosu@chem.ubbcluj.ro.

Notes

The authors declare no competing financial interest.

■ ACKNOWLEDGMENTS

This work was financially supported by ANR Blanc International DYNAMULTIREC (No. 13-IS07-0002-01) and CNCS-UEFISCDI (Project Nos. PN-II-ID-JRP-RO-FR-2012-0088 and PN-II-ID-PCCE-2011-2-0050).

■ REFERENCES

(1) Gazit, E. *Chem. Soc. Rev.* **2007**, *36*, 1263−1269.
(2) Zhang, S. *Nat. Biotechnol.* **2003**, *21*, 1171−1178.
(3) Bowden, N. B.; Weck, M.; Choi, I. S.; Whitesides, G. M. *Acc. Chem. Res.* **2001**, *34*, 231−238.
(4) Ben-Naim, A. *Int. J. Phys.* **2013**, *1*, 66−71.
(5) Clarkson, R. G.; Gomberg, M. J. *J. Am. Chem. Soc.* **1930**, *52*, 2881−2891.
(6) (a) Matuszna, K.; Breza, M.; Palszegi, T. *J. Mol. Struct.: THEOCHEM* **2008**, *851*, 277−283. (b) Lukeš, V.; Breza, M. *J. Mol. Struct.* **2004**, *699*, 93−99.
(7) (a) Schenk, H. *Acta Crystallogr., Sect. B: Struct. Crystallogr. Cryst. Chem.* **1972**, *B28*, 625−628. (b) Aujard, I.; Baltaze, J.-P.; Baudin, J.-B.; Cogné, E.; Ferrage, F.; Jullien, L.; Perez, E.; Prévost, V.; Qian, L. M.; Ruel, O. *J. Am. Chem. Soc.* **2001**, *123*, 8177−8188.
(8) Douthwaite, R. E.; Taylor, A.; Whitwood, A. C. *Acta Crystallogr., Sect. C: Cryst. Struct. Commun.* **2005**, *C61*, o328−o331.
(9) (a) Moreau, F.; Audebrand, N.; Poriel, C.; Moizan-Baslé, V.; Ouvry, J. *J. Mater. Chem.* **2011**, *21*, 18715−18722. (b) Laliberté, D.; Maris, T.; Demers, E.; Helzy, F.; Arseneault, M.; Wuest, J. D. *Cryst. Growth Des.* **2005**, *5*, 1451−1456. (c) Demers, E.; Maris, T.; Wuest, J. D. *Cryst. Growth Des.* **2005**, *5*, 1227−1235. (d) Demers, E.; Maris, T.; Cabana, J.; Fournier, J.-H.; Wuest, J. D. *Cryst. Growth Des.* **2005**, *5*, 1237−1245. (e) Wong, K.-T.; Liao, Y.-L.; Peng, Y.-C.; Wang, C.-C.; Lin, S.-Y.; Yang, C.-H.; Tseng, S.-M.; Lee, G.-H.; Peng, S.-M. *Cryst. Growth Des.* **2005**, *5*, 667−671. (f) Clews, P. K.; Douthwaite, R. E.; Kariuki, B. M.; Moore, T.; Taboada, M. *Cryst. Growth Des.* **2006**, *6*, 1991−1994. (g) Fournier, J.-H.; Maris, T.; Wuest, J. D. *J. Org. Chem.* **2004**, *69*, 1762−1775. (h) Darbost, U.; Cabana, J.; Demers, E.; Maris, T.; Wuest, J. D. *CheM* **2011**, *1*, 52−61.
(10) (a) Dawson, R.; Cooper, A. I.; Adams, D. J. *Prog. Polym. Sci.* **2012**, *37*, 530−563. (b) Kim, S.; Lee, Y. M. *Prog. Polym. Sci.* **2015**, *43*, 1−32. (c) Bezzu, C. G.; Carta, M.; Tonkins, A.; Jansen, J. C.; Bernardo, P.; Bazzarelli, F.; McKeown, N. B. *Adv. Mater.* **2012**, *24*, 5930−5933. (d) Takata, T.; Ishiwari, F.; Sato, T.; Seto, R.; Koyama, Y. *Polym. J. (Tokyo, Jpn.)* **2008**, *40*, 846−853. (e) Weber, J.; Thomas, A. *J. Am. Chem. Soc.* **2008**, *130*, 6334−6335.
(11) (a) Curiel, D.; Más-Montoya, M.; Sánchez, G. *Coord. Chem. Rev.* **2015**, *284*, 19−66. (b) Hovorka, R.; Hytteballe, S.; Piehler, T.; Meyer-Eppler, G.; Topić, F.; Rissanen, K.; Engeser, M.; Lützen, A. *Beilstein J. Org. Chem.* **2014**, *10*, 432−441. (c) Tejeda, A.; Oliva, A. I.; Simón, L.; Grande, M.; Cruz Caballero, M.; Morán, J. R. *Tetrahedron Lett.* **2000**, *41*, 4563−4566. (d) Das, G.; Hamilton, A. D. *Tetrahedron Lett.* **1997**, *38*, 3675−3678. (e) Hovorka, R.; Meyer-Eppler, G.; Piehler, T.; Hytteballe, S.; Engeser, M.; Topić, F.; Rissanen, K.; Lützen, A. *Chem. - Eur. J.* **2014**, *20*, 13253−3258. (f) Egli, M.; Dobler, M. *Helv. Chim. Acta* **1986**, *69*, 626−631. (g) Cuntze, J.; Owens, L.; Alcázar, V.; Seiler, P.; Diederich, F. *Helv. Chim. Acta* **1995**, *78*, 367−390. (h) Prelog, V. *Pure Appl. Chem.* **1978**, *50*, 893−904.
(12) (a) Bassani, D. M.; Jonusauskaite, L.; Lavie-Cambot, A.; McClenaghan, N. D.; Pozzo, J.-L.; Ray, D.; Vives, G. *Coord. Chem. Rev.* **2010**, *254*, 2429−2445. (b) Haick, H.; Cahen, D. *Prog. Surf. Sci.* **2008**, *83*, 217−261. (c) Valášek, M.; Edelmann, K.; Gerhard, L.; Fuhr, O.; Lukas, M.; Mayor, M. *J. Org. Chem.* **2014**, *79*, 7342−7357. (d) Wong, K.-T.; Chi, L.-C.; Huang, S.-C.; Liao, Y.-L.; Liu, Y.-H.; Wang, Y. *Org. Lett.* **2006**, *8*, 5029−5032. (e) Poriel, C.; Rault-Berthelot, J.; Barrière, F.; Slawin, A. M. Z. *Org. Lett.* **2008**, *10*, 373−376. (f) Jeon, N. J.; Lee, H. G.; Kim, Y. C.; Seo, J.; Noh, J. H.; Lee, J.; Seok, S. I. *J. Am. Chem. Soc.* **2014**, *136*, 7837−7840. (g) Romain, M.; Thiery, S.; Shirinskaya, A.; Declairieux, C.; Tondelier, D.; Geffroy, B.; Jeannin, O.; Rault-Berthelot, J.; Métivier, R.; Poriel, C. *Angew. Chem., Int. Ed.* **2015**, *54*, 1176−1180. (h) Wong, K.-T.; Liao, Y.-L.; Lin, Y.-T.; Su, H.-C.; Wu, C.-C. *Org. Lett.* **2005**, *7*, 5131−5134. (i) Romain, M.; Tondelier, D.; Vanel, J.-C.; Geffroy, B.; Jeannin, O.; Rault-Berthelot, J.; Métivier, R.; Poriel, C. *Angew. Chem., Int. Ed.* **2013**, *52*, 14147−14151. (j) Horhant, D.; Liang, J.-J.; Virboul, M.; Poriel, C.; Alcaraz, G.; Rault-Berthelot, J. *Org. Lett.* **2006**, *8*, 257−260. (k) Jiang, Z.; Yao, H.; Zhang, Z.; Yang, C.; Liu, Z.; Tao, Y.; Qin, J.; Ma, D. *Org. Lett.* **2009**, *11*, 2607−2610. (l) Thiery, S.; Tondelier, D.; Declairieux, C.; Geffroy, B.; Jeannin, O.; Métivier, R.; Rault-Berthelot, J.; Poriel, C. *J. Phys. Chem. C* **2015**, *119*, 5790−5805. (m) Lai, M.-Y.; Chen, C.-H.; Huang, W.-S.; Lin, J. T.; Ke, T.-H.; Chen, L.-Y.; Tsai, M.-H.; Wu, C.-C. *Angew. Chem., Int. Ed.* **2008**, *47*, 581−585. (n) Lin, Y.; Chen, Z.-K.; Ye, T.-L.; Dai, Y.-F.; Ma, D.-G.; Ma, Z.; Liu, Q.-D.; Chen, Y. *Polymer* **2010**, *51*, 1270−1278. (o) Liaptsis, G.; Hertel, D.; Meerholz, K. *Angew. Chem., Int. Ed.* **2013**, *52*, 9563−9567.
(13) (a) Steiner, T. *Chem. Commun.* **1997**, *8*, 727−734. (b) Desiraju, G. R. *Angew. Chem., Int. Ed.* **2007**, *46*, 8342−8356.
(14) Salbeck, J.; Lupo, D. *Pat. Appl.* US20030111107A1, 2003.
(15) (a) Wuest, J. D. *Chem. Commun.* **2005**, 5830−5837. (b) Chun, J.; Kang, S.; Park, N.; Park, E. J.; Jin, X.; Kim, K.-D.; Seo, H. O.; Lee, S. M.; Kim, H. J.; Kwon, W. H.; Park, Y.-K.; Kim, J. M.; Kim, Y. D.; Son, S. U. *J. Am. Chem. Soc.* **2014**, *136*, 6786−6789. (c) Yuan, D.; Lu, W.; Zhao, D.; Zhou, H.-C. *Adv. Mater.* **2011**, *23*, 3723−3725.
(16) Lions, F.; Martin, K. V. *J. Am. Chem. Soc.* **1957**, *79*, 2733−2738.
(17) Legrand, Y. M.; Dumitru, F.; van der Lee, A.; Barboiu, M. *Supramol. Chem.* **2009**, *21*, 230−237.
(18) Morimoto, T.; Uno, H.; Furuta, H. *Angew. Chem., Int. Ed.* **2007**, *46*, 3672−3675.
(19) (a) Dumitru, F.; Petit, E.; van der Lee, A.; Barboiu, M. *Eur. J. Inorg. Chem.* **2005**, 4255−4262. (b) Dumitru, F.; Legrand, Y. M.; van der Lee, A.; Barboiu, M. *Chem. Commun.* **2009**, 2667−2669.
(20) (a) Langs, D. A. *Science* **1988**, *241*, 188−191. (b) Cohen, C. *J. Struct. Biol.* **1998**, *122*, 3−16. (c) Creager, A. N. *The Life of a Virus: Tobacco Mosaic Virus as an Experimental Model*; University of Chicago Press: Chicago, 2002.

DOI: 10.1021/acs.orglett.5b01576
Org. Lett. 2015, 17, 3494−3497